



Application of m-CNTs/NaClO₄/Ppy to a fast response, room working temperature ethanol sensor

Ren-Jang Wu^{a,*}, Yu-Ching Huang^a, Ming-Ru Yu^a,
Tzu Hsuan Lin^b, Shih-Lin Hung^b

^a Department of Applied Chemistry, Providence University, 200 Chungchi Road, Shalu, Taichung, Hsien 433, Taiwan, ROC

^b Department of Civil Engineering, National Chiao Tung University, Hsinchu 300, Taiwan, ROC

ARTICLE INFO

Article history:

Received 2 February 2008

Received in revised form 19 April 2008

Accepted 23 April 2008

Available online 30 April 2008

Keywords:

Polypyrrole

Multiwall carbon nanotubes (m-CNTs)

UV-photo polymerization

Ethanol sensor

ABSTRACT

A new blended material, m-CNTs/NaClO₄/Ppy, was developed as a gas sensor to detect ethanol concentrations at room temperature. The sensing material polypyrrole (Ppy) was synthesized *in situ* by UV-photo-polymerization. The multiwall carbon nanotubes (m-CNTs) added enhanced the short-term repeatability of the Ppy-sensing material. The relative resistance variation ($R_{\text{ethanol}}/R_{\text{air}}$) of m-CNTs/NaClO₄/Ppy was 1.193 when exposed to ethanol of 30,000 ppm. The sensor response and recovery times (both 20 s) were very short to this concentration. An unstable baseline of the sensor was explained by theoretical calculation of molecular dynamics made for ethanol adsorption on polypyrrole, which revealed formation of a new bond, N–H···O. Adsorption energy decreased with increasing the number of ethanol molecules adsorbed and was 0.8 kcal/mol at eight adsorbed molecules. Sensor responses of three different Ppy samples were measured to ethanol concentrations of 18,000–40,000 ppm.

© 2008 Elsevier B.V. All rights reserved.

1. Introduction

Ethanol concentration detectors have wide applications in many fields such as traffic safety, foodstuffs, fermentation processes, and alcoholic beverage production processes. Several different sensing technologies, including electrochemical [1], optical [2], and resistive [3–13], have been used to detect ethanol concentrations. Among the various types of sensors, the resistive method has the advantages of simplicity of construction and low cost, and popular applications.

SnO₂ is often used as an ethanol sensor, but generally it requires a high working temperature exceeding 300 °C. Long and Tsai found the optimum temperature of 350 °C for the SnO₂ material to response to alcohol of 3000 ppm, the sensor response S (relative resistance variation, $S = R_{\text{air}}/R_{\text{alcohol}}$) being about 9–10. They also found that the sensing properties were promoted by addition of some metal oxides. The addition of CaO decreased the response time, while an appropriate amount of SiO₂ doping increased the stability. In recent years many researchers have sought ethanol-sensing materials that could work at room temperature to save power and reduce the cost of the end devices. Wang et al. [4] fabricated a thin film SnO₂-sensing

material which had a very fast response time. Melo et al. [5] used the blended materials of poly(caprolactone), poly(ethylene oxide) (PEO), poly(methylmethacrylate), poly(vinyl alcohol) (PVA), poly(vinyl acetate), and polypyrrole (Ppy) materials to detect volatile organic compounds (VOCs), and obtained the sensor responses range from 5.5 to 7 with a PEO–Ppy material under highly pure ethanol vapor conditions. Jiang et al. [6] applied Ppy–PVA to measure methanol vapor from 49 to 1059 ppm, and the sensor response obtained was $S = 1.03$ – 1.07 [6]. On the other hand, Mills et al. [7] coated a quartz crystal microbalance (QCM) with array-type polymer sensing materials, and measured the oscillating frequency variation upon ethanol adsorption; the sensor signal ($S = \Delta f/\text{Hz}$) was 58 Hz in 320 ppm ethanol when used poly(vinylpyrrolidone) (PVPyr), Poly(ethylene-co-methylacrylate) (PE-co-MA), poly(vinylphenylketone) (PVPK), poly(vinyl chloride) (PVC), Poly(methyl methylacrylate) (PMMA), poly(ethylene-co-vinyl acetate) (PE-co-VA) and poly(styrene) (PS).

Carbon nanotubes (CNTs) are a useful and active material that could be used in various forms of chemical detection [8–20], and they possess many good properties. The sorptive property of CNTs is an important factor for its sensing behavior [8]. Composite materials of chitosan-CNTs are chosen as lactate sensors [9]. CNTs are the essential component of the composite sensors, and they are thought to behave as a cross-linking material [10]. Multiwall carbon nanotubes (m-CNTs) are grown on a silicon nanoporous platform and used as a humidity sensor [11]. The sensor device is

* Corresponding author. Tel.: +886 4 26328001/15212; fax: +886 4 26327554.
E-mail address: rjwu@pu.edu.tw (R.-J. Wu).

demonstrated to be highly repeatable [8]. CNTs are also employed as a promotive additive for detection of NH_3 and NO_2 gases, volatile organic compounds, and biomaterials [12–20].

In this study, a significant enhancement in sensor response stability and a reduction in response time were found at low ethanol concentrations with the addition of m-CNTs to NaClO_4 -Ppy, in comparison with the Ppy material alone. The new materials possess the benefits of operation at room temperature, easily fabrication, and low cost as an ethanol-sensing device.

2. Experimental

All the chemicals used were of analytical reagent (AR) grade (purity >99%) and were purchased from Sigma-Aldrich Co. Inc., USA. All the chemicals were used as received. Water was distilled and de-ionized (DI) using a Milli-Q water purification system (Millipore Corp.).

2.1. Preparation of sensing material and sensor head

0.07 g of monomer pyrrole (Py) was added to 100 ml of ethyl alcohol to form a solution. 0.01 g of AgNO_3 was added to the solution and stirred thoroughly, distributing it equally throughout the Py alcohol matrix and making it available for initiating photo-polymerization [21]. The additive AgNO_3 usually acts as a promoter for absorption of light. One weight percentage of NaClO_4 against Py was added to the solution and homogenized to form a NaClO_4 + Py solution. Ozone-UV treatment was conducted by placing m-CNTs in a beaker which was to fill with ozone under UV light for 5 h. Further, they were modified by aggressive breakup to open the closed ends. One weight percentage m-CNTs were added into the NaClO_4 + Py mixtures to form an m-CNTs + NaClO_4 + Py solution.

Subsequently, a substrate chip was dip coated with the various mixed solutions of Py, NaClO_4 + Py and m-CNTs + NaClO_4 + Py. The dipping and withdrawing speed of the substrate were about 3 and 5 cm/s, respectively. The chip was made of an alumina substrate (10 mm × 5 mm), and a pair of comb-like interdigitated gold electrodes were screen printed on it, followed by UV treatment for 5 h to photo polymerize the Py coating at room temperature.

2.2. Sensing system

The test gas concentration was controlled using two mass flow controllers (MFCs), as shown in Fig. 1. Within the test system, the

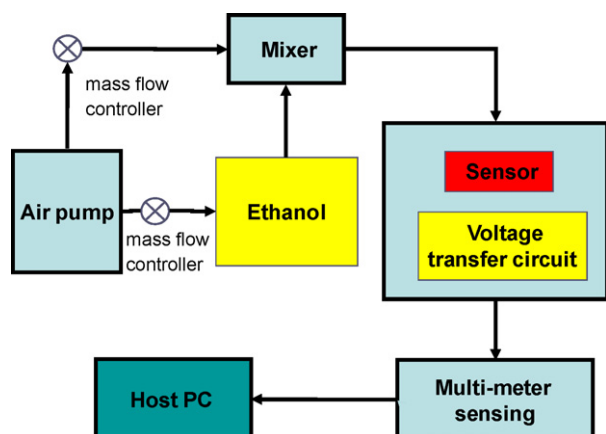


Fig. 1. Experiment setup.

concentration of ethanol varied from 18,000 to 40,000 ppm. One of the MFCs regulated the flow rate of dry air and another was used for volatile ethanol. The flow rate of the test gas was fixed at 1000 cm^3/min during measurement. Dry air and volatile ethanol were mixed in a chamber and flowed up to the sensor chip. Acetone used as an interference gas. Once the gas was in contact with the sensor chip, a change in sensor signal was seen (either resistance or voltage) corresponding to the concentration of ethanol. Subsequently, the connected multi-meter sensing unit transmitted the signal to a host PC. All sensing experiments were done at $24.5 \pm 0.5^\circ\text{C}$, and humidity was kept at $60 \pm 5\%$ RH.

A simple voltage circuit was used to measure the sensor resistance [22] with an input voltage of 2.0V. The sensor response was defined as $S = R_{\text{ethanol}}/R_{\text{air}}$, where R_{ethanol} and R_{air} were the resistances in an environmental containing ethanol and in air, respectively.

2.3. UV-vis testing and SEM

The obtained Ppy was investigated using UV-vis spectroscopy to verify the completion of polymerization. The UV-vis spectrometer used here was SINCO, SUV-2100 series (<http://www.scinco.com>; Korea). Light sources for the UV-vis were deuterium and tungsten-halogen lamps, respectively, and the wavelengths scanned ranged from 200 to 700 nm. The morphology and thickness of the samples were obtained with a JEOL scanning electron microscope (SEM model number: JSM-6500), using an accelerating voltage of 5–15 kV.

2.4. Theoretical analysis

A series of molecular dynamics/simulations calculated the bonding energy for ethanol molecule adsorption onto the Ppy surface using Materials Studio[®], Version 3.2 (Accelrys Software Inc., <http://www.accelrys.com/products/mstudio/>). By applying the discovery method of the software, the parameters were chosen to minimize the system energy, and the compass force field was used [21].

At first, the homopolymer function was set up and the parameters of polymerization of polypyrrole were built. The related conditioned parameters chosen were rings library, pyrrole repeated unit, isotactic tacticity, three chain length, and six chain number. The lattice parameters of polypyrrole were set at the 3D triclinic without constraint. From the initial to final potential energy change during the process of calculation, the final potential energy was chosen. This term refers to the most stable structure of the adsorbed molecule and Ppy surface system. According to the simulation of the adsorption on the Ppy surface, the bond length and energy of the new conformation can be determined.

3. Results and discussion

3.1. UV-vis spectra of samples

UV-vis spectra of various pyrrole samples are given in Fig. 2. The peak of the pyrrole band was at 250 nm after UV treatment was done at room temperature for 5 h to allow photo-polymerization to occur. Broad peaks of various samples were seen over a range of 400–500 nm, indicating the completion of polymerization of Py to Ppy. This explains why pyrrole monomers were polymerized into polypyrrole. Thus, the obtained prominent absorption peak at 470 nm is due to the electronic transition of π - π^* bonds in Ppy [21]. The 470 nm peak of the m-CNTs/ NaClO_4 /Ppy sample is the strongest of all the samples. This reveals that the addition of m-CNTs helps the polymerization of Py to Ppy. The m-CNTs could help

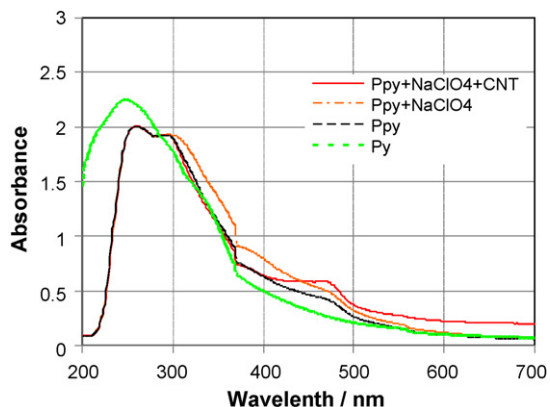


Fig. 2. UV-vis spectra of various Ppy samples.

the polymerization by two ways. One is that m-CNTs as a template offer a place for photo-polymerization. Another is that after the UV and ozone treatment, some functional groups are produced on the neighborhood of open end and wall side surface [23,24]. It represents that more Py molecules could be attached and go through the polymerization.

3.2. SEM figure of m-CNTs/NaClO₄/Ppy

SEM and TEM images of the m-CNTs material are shown in Fig. 3. They reveal some fiber-like wires and some bundles about 20–40 nm in diameter. Comparing the SEM and TEM images in Fig. 3(a) and (b), after treatment more m-CNTs were broken and the fractured end surfaces provided more possibility to bind with Ppy. The SEM image of the top view in Fig. 4(a) reveals the existence of some particles of material. This is hydrated NaClO₄ on the Ppy surface after the 5-h polymerization, and m-CNTs were not found on the surface of the film. It is proposed that the m-CNTs were embedded in the bulk of Ppy. The thickness of the Ppy film was estimated as 3–5 μm for 5 h photo-polymerization according to the side view in Fig. 4(b).

3.3. Adsorption of ethanol on the Ppy surface

The local geometry for ethanol molecules adsorbed on the Ppy surface is shown in Fig. 5, which indicates that the oxygen atom of ethanol is bonded to the H atom of Ppy. According to the calculation of ethanol adsorbed on Ppy, the new bonding of N–H···O could be formed. According to the Molecular dynamics calculation, the O···H bond length is 0.194 nm. It is shown in Fig. 5 that the most stable distance is 0.194 nm. The distance is related to the lowest potential

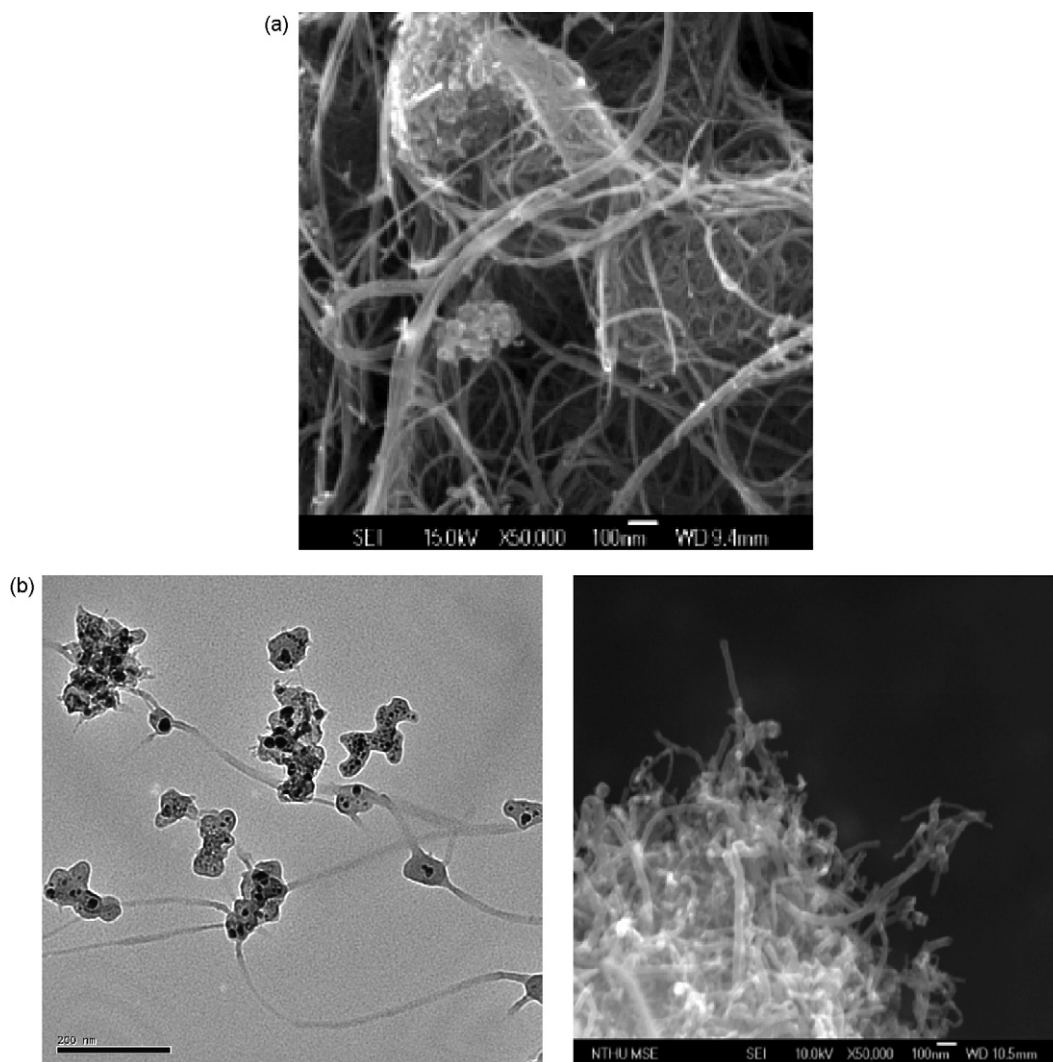


Fig. 3. SEM and TEM images of m-CNTs: (a) SEM images before UV/ozone treatment, (b) TEM (left) and SEM (right) images after UV/ozone treatment.

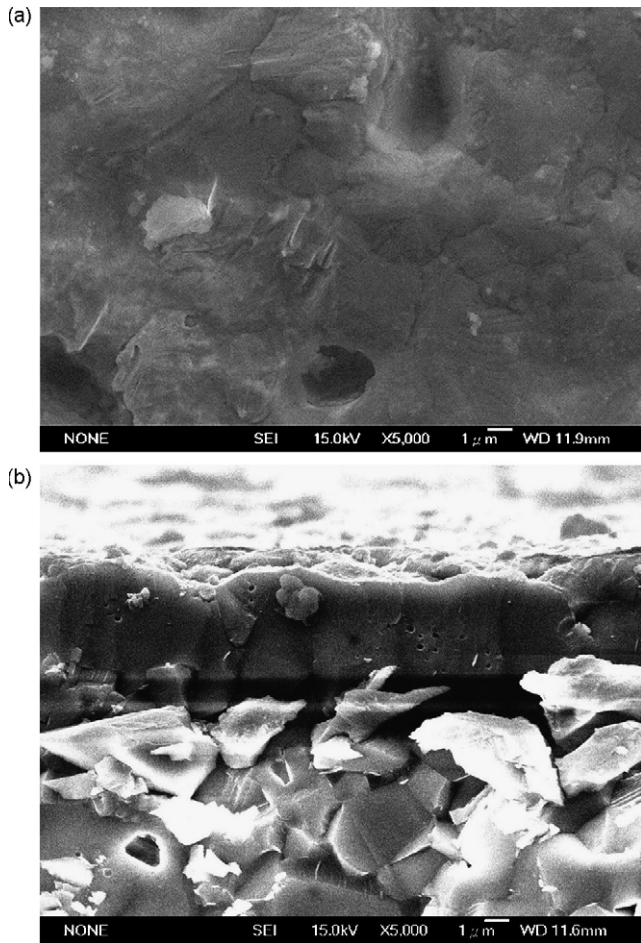


Fig. 4. SEM images of an m-CNTs/NaClO₄/Ppy film on an alumina substrate: (a) top view and (b) side view.

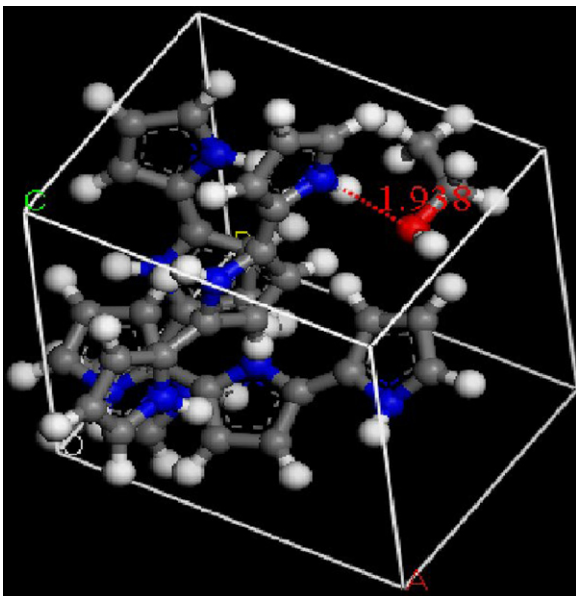
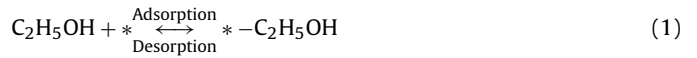


Fig. 5. Simulation of ethanol adsorption on the Ppy surface. White balls represent hydrogen atoms, deep blue balls nitrogen atoms, and red balls oxygen atoms.

energy of the suitable dynamic range of 0.18–0.21 nm [21]. Ethanol adsorption, represented in Eq. (1), on a vacant site of polypyrrole (represented by *) was calculated as an exothermic process.



While an ethanol molecule was adsorbed on the 3×3 Ppy surface, in theory, the bond energy was calculated as -15.8 kcal/mol, and the interaction of ethanol and Ppy was assigned as a chemical bond on the surface. Therefore irreversible adsorption occurred on the Ppy surface, so that the background signals of the ethanol sensor in Fig. 6(a) were not stable. If more than one ethanol molecule were adsorbed on the 3×3 Ppy surface, the bond energy decreased as the adsorbed ethanol molecules increased, as shown in Fig. 7. When eight molecules were adsorbed, the adsorption energy decreased to 0.8 kcal/mol, and thus the energy approached to the nature of van der Waals force.

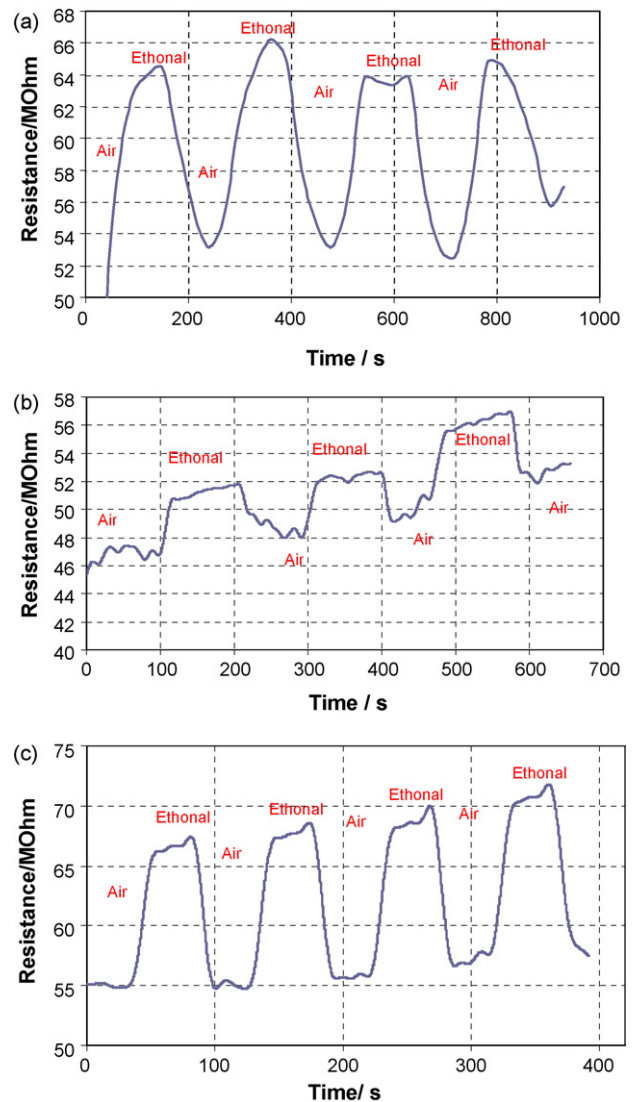


Fig. 6. Sensing transients to 30,000 ppm ethanol of (a) Ppy, (b) NaClO₄/Ppy, and (c) m-CNTs/NaClO₄/Ppy.

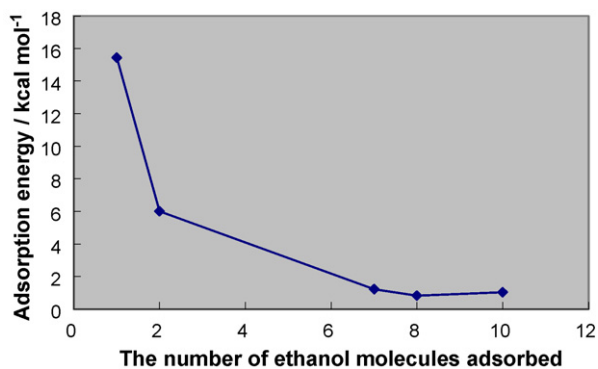


Fig. 7. Exothermic adsorption energy of each ethanol molecule on Ppy surface.

3.4. Ethanol-sensing characteristics

Fig. 6 shows the sensing characteristics when 30,000 ppm ethanol gas was adsorbed on the surface of Ppy, NaClO₄/Ppy and m-CNTs/NaClO₄/Ppy. According to the molecular dynamics calculation the ethanol was adsorbed on the Ppy, and the oxygen atom of ethanol bonded to the hydrogen atom of pyrrole. The oxygen atom possesses high electronegativity and can withdraw electrons from hydrogen atoms in Ppy, decreasing the electron density of Ppy and thus increasing the surface resistance of Ppy. Fig. 6(a)–(c) also demonstrate that the resistance increased with the change in ethanol concentration in the chamber. The data of Fig. 6(a) reveals that the sensor response baseline of the Ppy film was not stable. According to our above calculation in Section 3.3, this might arise from the fact that some irreversible adsorption occurred on the Ppy surface. The m-CNTs with n-type semiconductor type characteristics [20] donate electrons to Ppy and weaken the O–H bond of Fig. 5 [14]. This is the reason why the addition m-CNTs can reduce the adsorption energy on the Ppy surface. Comparison Fig. 6(a) and (c) make it clear that the sensor response baseline of m-CNTs/NaClO₄/Ppy was more stable than Ppy. The addition of m-CNTs makes the adsorption and desorption of ethanol molecules reversible on Ppy. It also results in a more stable baseline of the sensor response signals. Under 30,000 ppm concentration conditions, the sensor response of m-CNTs/NaClO₄/Ppy was $S = 1.193$. Comparing Fig. 6(a) and (b), the resistance of NaClO₄/Ppy is lower than the Ppy material. For the ionic property of NaClO₄, the function of NaClO₄ is to increase the conductivity value of the Ppy-sensing material.

3.5. Response time, recovery time and interference

In Table 1, the response time T_{90} of 30,000 ppm ethanol gas sensing is 50 s in the Ppy film, and adding NaClO₄ and m-CNTs can shorten the response time. This might be because the addi-

Table 1
Sensor response, response and recovery times to ethanol of 30,000 ppm and an interference effect of acetone

	Ppy	Ppy/NaClO ₄	m-CNTs/Ppy/NaClO ₄
Sensor response	1.24	1.14	1.19
T_{90}	50 s	10 s	20 s
T_{r90}	40 s	10 s	20 s
Sensor response of acetone in 54,000 ppm	–	–	1.02
T_{90}	–	–	320 s
T_{r90}	–	–	270 s

T_{90} (response time) represents the time to reach 90% of the equilibrium signal. T_{r90} (recovery time) represents the time to back to 90% of the background signal.

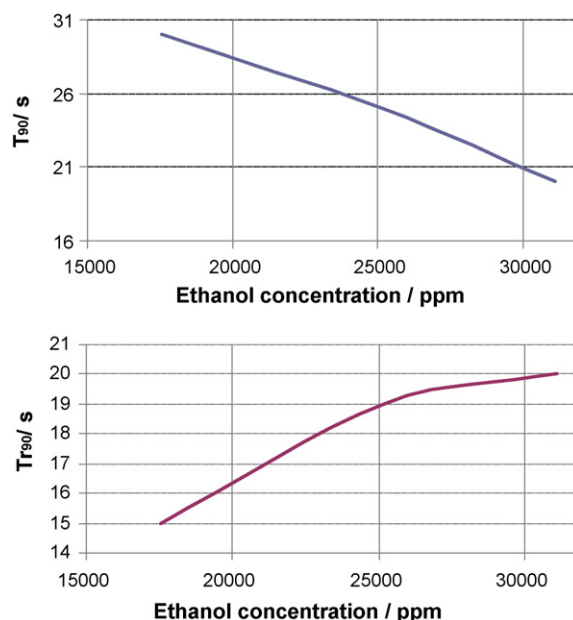


Fig. 8. Response and recovery times (T_{90} and T_{r90} see footnotes in Table 1) as a function of ethanol concentration.

tion of NaClO₄ and m-CNTs reduces the adsorption energy on the Ppy surface. In Fig. 8, the response time of the m-CNTs/NaClO₄/Ppy decreased with increasing the concentration. From the results of Fig. 7, the adsorption and desorption of a large number of ethanol molecules are the type of reversible in physisorption on m-CNTs/NaClO₄/Ppy. Thus, the response and recovery time of the ethanol sensor are fast. Table 1 reveals that the interference of acetone gas was very little and the sensor response was $S = 1.02$ to 54,000 ppm acetone.

3.6. Response magnitude versus ethanol concentration

Varying the ethanol concentration from 18,000 to 40,000 ppm, we rendered the sensor response versus concentration curves in Fig. 9. Repeatability of the sensor response was tested thrice at each concentration and the relative standard deviation ranged from 7.2 to 11.3%. Ppy was not relatively sensitive to the concentration variation due to the saturation adsorption of ethanol [22]. The sensing material of m-CNTs/NaClO₄/Ppy then possessed the highest sen-

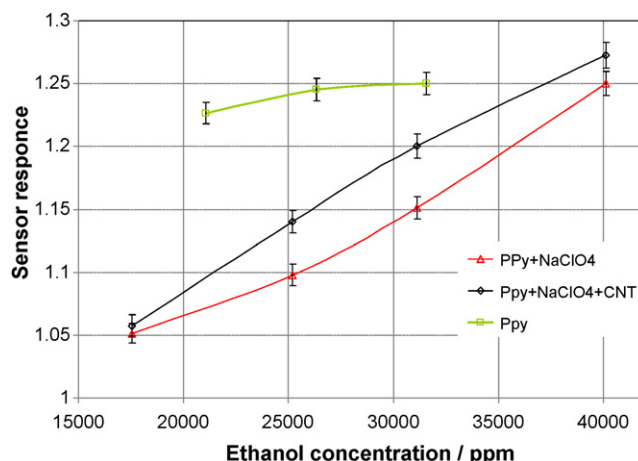


Fig. 9. Comparison of sensor responses of various Ppy films.

sitivity (Δ sensor response/ Δ ethanol concentration), and thus it holds great promise as a sensing material for ethanol detection. The range of ethanol detection is from 18,000 to 40,000 ppm, and the range is relatively high. The benefits of this sensor are the operation at room temperature, easily fabrication and low cost of mass production, compared with the conventional sensors (it needs working temperature of several hundred degree of Celsius).

4. Conclusions

A blended material of m-CNTs/NaClO₄/Ppy was fabricated by UV-photo-polymerization for ethanol sensing at room temperature. The adsorption energy decreased as the number of adsorbed molecules increased, and reached down to 0.8 kcal/mol when eight molecules were adsorbed, the energy being near to van der Waals force. The blended material, m-CNTs/NaClO₄/Ppy, possessed a higher sensor response than NaClO₄/Ppy or pure Ppy. The response to 30,000 ppm ethanol of the m-CNTs/NaClO₄/Ppy was $S = 1.193$. The sensor response and recovery times (both 20 s) were very short to an ethanol concentration of 30,000 ppm. Molecular dynamics calculation made for ethanol adsorption on Ppy revealed formation of a new bond, N–H...O. The measurements of sensor responses of three different Ppy samples to ethanol of 18,000–40,000 ppm revealed that m-CNTs/NaClO₄/Ppy possesses the highest sensitivity.

References

- [1] J.J. Huang, W.S. Hwang, Y.C. Weng, T.C. Chou, Determination of alcohols using a Ni–Pt alloy amperometric sensor, *Thin Solid Films*, in press.
- [2] K. Mitsubayashi, T. Kon, Y. Hashimoto, Optical bio-sniffer for ethanol vapor using an oxygen-sensitive optical fiber, *Biosens. Bioelectron.* 19 (2003) 193–198.
- [3] T.R. Ling, C.M. Tsai, Influence of nano-scale dopants of Pt, CaO and SiO₂, on the alcohol sensing of SnO₂ thin films, *Sens. Actuators B: Chem.* 119 (2006) 497–503.
- [4] H.C. Wang, Y. Li, M.J. Yang, Fast response thin film SnO₂ gas sensors operating at room temperature, *Sens. Actuators B: Chem.* 119 (2006) 380–383.
- [5] C.P. Melo, B.B. Neto, E.G. Lima, L.F.B. Lira, J.E.G. Souza, Use of conducting polypyrrole blends as gas sensors, *Sens. Actuators B: Chem.* 109 (2005) 348–354.
- [6] L. Jiang, H.K. Jun, Y.S. Hoh, J.O. Lim, D.D. Lee, J.S. Huh, Sensing characteristics of polypyrrole-poly(vinyl alcohol)methanol sensors prepared by in situ vapor state polymerization, *Sens. Actuators B: Chem.* 105 (2005) 132–137.
- [7] C.A. Mills, J. Beeley, C. Wyse, D.R.S. Cumming, A. Gildle, J.M. Cooper, Polymer-based micro-sensor paired arrays for the determination of primary alcohol vapors, *Sens. Actuators B: Chem.* 125 (2007) 85–91.
- [8] J. Kong, N.R. Franklin, C. Zhou, M.G. Chapline, S. Peng, K. Cho, H. Dai, Nanotube molecular wires as chemical sensors, *Science* 287 (2000) 622–625.
- [9] R.H. Baughman, C. Cui, A.A. Zakhidov, Z. Iqbal, J.N. Barasci, G.M. Spinks, G.G. Wallace, A. Mazzoldi, D. de Rossi, A.G. Rinzier, O. Jaschinski, S. Roth, M. Kertesz, Carbon nanotube actuators, *Science* 284 (1999) 1340–1342.
- [10] J. Fan, M. Wan, D. Zhu, B. Chang, Z. Pan, S. Xie, Synthesis, characterizations, and physical properties of carbon nanotubes coated by conducting polypyrrole, *J. Appl. Polym. Sci.* 74 (1999) 2605–2610.
- [11] Q. Ameer, S.B. Adeloju, Polypyrrole-based electronic noses for environmental and industrial analysis, *Sens. Actuators B: Chem.* 106 (2005) 541–552.
- [12] P. Rapta, R. Faber, L. Dunsch, A. Neudeck, O. Nuyken, In situ EPR and UV–vis spectroelectrochemistry of hole-transporting organic substrates, *Spectrochim. Acta A* 56 (2000) 357–362.
- [13] Y. Shen, M. Wan, In situ doping polymerization of pyrrole with sulfonic acid as a dopant, *Syn. Met.* 96 (1998) 127–132.
- [14] M. Trojanowicz, Analytical applications of carbon nanotubes: a review, *TrAC Trends in Anal. Chem.* 25 (2006) 480–489.
- [15] X. Cui, C.M. Li, J. Zang, S. Yu, Highly sensitive lactate biosensor by engineering chitosan/PVI-Os/M-CNTS/LOD network nanocomposite, *Biosens. Bioelectron.* 22 (2007) 3288–3292.
- [16] W.F. Jiang, S.H. Xiao, C.Y. Feng, H.Y. Li, X.J. Li, Resistive humidity sensitivity of arrayed multi-wall carbon nanotube nests grown on arrayed nanoporous silicon pillars, *Sens. Actuators B: Chem.* 125 (2007) 651–655.
- [17] L.H. Nguyen, T.V. Phi, P.Q. Phan, H.N. Vu, C.N. Duc, F. Fossard, Synthesis of multi-walled carbon nanotubes for NH₃ gas detection, *Physica E* 37 (2007) 54–57.
- [18] R.K. Roy, M.P. Chowdhury, A.K. Pal, Room temperature sensor based on carbon nanotubes and nanofibres for methane detection, *Vacuum* 77 (2005) 223–229.
- [19] S. Peng, K. Cho, P. Qi, H. Dai, Ab initio study of M-CNTS NO₂ gas sensor, *Chem. Phys. Lett.* 387 (2004) 271–276.
- [20] B.Y. Wei, M.C. Hsu, P.G. Su, H.M. Lin, R.J. Wu, H.J. Lai, A novel SnO₂ gas sensor doped with carbon nanotubes operating at room temperature, *Sens. Actuators B: Chem.* 101 (2004) 81–89.
- [21] R.J. Wu, Y.C. Huang, M. Chavali, T.H. Lin, S.L. Hung, H.N. Luk, New sensing technology for detection of the common inhalational anesthetic agent sevoflurane using conducting polypyrrole films, *Sens. Actuators B: Chem.* 126 (2007) 387–393.
- [22] R.J. Wu, C.Y. Chen, M.H. Chen, Y.L. Sun, Photoreduction measurement of ozone using Pt/TiO₂–SnO₂ material at room temperature, *Sens. Actuators B: Chem.* 123 (2007) 1077–1082.
- [23] X.D.L. Wang, T. Sun, J. Zhou, Q. Yang, Study on ethylene polymerization catalyzed by Cp₂ZrCl₂/carbon nanotube system, *J. Mol. Catal. A: Chem.* 255 (2006) 10–15.
- [24] V. Selvaraj, M. Alagar, K.S. Kumar, Synthesis and characterization of metal nanoparticles-decorated Ppy–m-CNTS composite and their electrocatalytic oxidation of formic acid and formaldehyde for fuel cell applications, *Appl. Catal. B: Environ.* 75 (2007) 129–138.

Biographies

Ren-Jang Wu is an associate professor in Providence University. He received a BS in Chemistry from National Tsinghua University in 1986, an MS in Chemistry from National Taiwan University in 1988, and a PhD in Chemistry from National Tsinghua University in 1995. He is interested in chemical sensors, catalysis, nanoscience, and chemical standards technology.

Yu-Ching Huang received a BS in Chemistry from Providence University in 2004 and an MS in Chemistry from Providence University in 2007. His interests are theoretical calculations for adsorption and desorption of the sensing material surface on chemical sensors.

Ming-Ru Yu received a BS in Chemistry from Providence University in 2006. He is interested in fabricating nanomaterials and chemical sensor technology.

Tzu Hsuan Lin received his MSc (Tech.) in Civil Engineering from National Chiao Tung University in 2003. From 2005 he attended to a doctoral program in National Chiao Tung University. His interests are wireless sensor networks, RFID technology, and structural health monitoring.

Shih-Lin Hung is a professor in National Chiao Tung University. He received a BS in Civil Engineering from National Chiao Tung University in 1982, an MS in Civil Engineering from Ohio State University in 1990, and a PhD in Civil Engineering from Ohio State University in 1992. His present research focuses on wireless sensor networks, ANN, structure monitoring, and wavelets.